Structure Elucidation of Sphingolipids from the Mycopathogen *Paracoccidioides brasiliensis*: An Immunodominant β-Galactofuranose Residue Is Carried by a Novel Glycosylinositol Phosphorylceramide Antigen†

Steven B. Levery,*,‡ Marcos S. Toledo,§ Anita H. Straus,§ and Helio K. Takahashi§

University of Georgia/Complex Carbohydrate Research Center, 220 Riverbend Road, Athens, Georgia 30602, and Department of Biochemistry, Universidade Federal de Sao Paulo/Escola Paulista Medicina, Rua Botucatu 862, 04023-900, Sao Paulo, SP, Brazil

Received December 8, 1997; Revised Manuscript Received April 6, 1998

ABSTRACT: Two major acidic glycolipid components (Pb-**1** and Pb-**2**) have been extracted from the mycopathogen *Paracoccidioides brasiliensis*, a thermally dimorphic fungus endemic to rural areas of South and Central America. Sera of all patients exhibiting paracoccidioidomycosis were found to be reactive with Pb-**1**, but not with Pb-**2**; no reactivity was observed with sera of healthy patients or those with histoplasmosis [Toledo, M. S., Suzuki, S., Straus, A. H., and Takahashi, H. K. (1995) *J. Med. Vet. Mycol. 33*, 247−251]. We report here the complete structure elucidation of both *P. brasiliensis* glycolipids using monosaccharide, fatty acid, sphingosine, and inositol component analysis by GC-MS; ^{1}H- and ^{31}P NMR spectroscopy; ESI-MS and -MS/CID-MS, linkage analysis, and exoglycosidase digestion. The compounds were found to be glycosylinositol phosphorylceramides (GIPCs) with the following structures: Pb-**2**, Man*p*α1→3Man*p*α1→2Ins1-P-1Cer; and Pb-**1**, Man*p*α1→3[Gal*f*β1→6]Man*p*α1→2Ins1-P-1Cer. The serologically nonreactive Pb-**2** appears to be a biosynthetic intermediate between mannosylinositol phosphorylceramide (MIPC), which is widely distributed among fungi, and the antigenic Pb-**1**. Pb-**1** is a novel glycosphingolipid, similar to a triglycosyl IPC (Hc-**VI**) reported from *Histoplasma capsulatum* [Barr, K., Laine, R.A, and Lester, R. L. (1984) *Biochemistry 23*, 5589−5596], but differing in the anomeric configuration of the terminal Gal*f*1→6 residue, which is immunodominant. The significance of these structures as serological and taxonomic markers, as well as their potential utility as targets for immunodiagnostic agents, is discussed.

Although glycosphingolipids appear to be ubiquitous components of eukaryotic cells, they vary widely in both glycan and ceramide structure, depending on phylum, species, tissue, stage of differentiation and development, and pathology (*3*). In humans, even individuals may be characterized by distinctive glycosphingolipid distribution patterns expressed on various tissues. Phylogenetically related organisms may synthesize similar glycan or ceramide structures distinct from those found in other classes of organism; on the other hand, some structures, such as simple glucosyl- and galactosylceramides (cerebrosides), are widely distributed among various phyla, including mammals, invertebrates, and fungi (*3*−*5*); in some cases these may also exhibit fairly common fatty acid or sphingosine components, while in others, one or both of these components may be quite unusual [e.g., the 9-methyl-4,8,10-sphingatriene reported for cerebrosides of the sea star *Ophidiaster ophidiamus* (*6*)].

Compounds based on glycosylation of *myo*-inositol-(1-*O*-phosphoryl-1)ceramide (InsPCer or IPC[1]) form a special class of glycosphingolipids found in plants, yeasts, filamentous fungi, and protozoans, but so far not in animal cells, which apparently lack the capacity to synthesize IPC (*7*). Among yeasts and filamentous fungi, extractable[2] GIPCs have been identified in *Saccharomyces cerevisiae*, *Cryptococcus neoformans*, *Candida* spp. (*albicans* and *utilis*), *Aspergillus niger*, and *Histoplasma capsulatum* (for review, see refs *4*, *7*; see also refs *8*, *9*). Only nonglycosylated IPCs have been extracted from the phytopathogenic *Phytophthora* spp. (*capsici* and *parasitica*) (*10*−*12*), while only IPC and $(IP)_2C$ were found in *Neurospora crassa* (*13*). Aside from the well-

† This work was supported by the National Institutes of Health Resource Center for Biomedical Complex Carbohydrates (NIH #5 P41 RR05351; S.B.L.); and by FAPESP, CNPq, and PRONEX (Brazil; M.S.T., A.H.S., and H.K.T.).

* Author to whom correspondence should be addressed.
‡ University of Georgia/Complex Carbohydrate Research Center.
§ Universidade Federal de Sao Paulo/Escola Paulista Medicina.

[1] Abbreviations: FAME, fatty acid methyl ester; GIPC, glycosylinositol phosphorylceramide; IPC, inositol phosphorylceramide; MIPC, mannosylinositol phosphorylceramide; PMAA, partially methylated alditol acetate; TMS, trimethylsilyl; HPLC, high-performance liquid chromatography; HPTLC, high-performance thin-layer chromatography; GC, gas chromatography; MS, mass spectrometry; EI, electron impact ionization; ESI, electrospray ionization; FAB, fast atom bombardment; CID, collision induced decomposition; MSD, mass selective detector; NMR, nuclear magnetic resonance; PD, preparatory delay; PS, phase sensitive; DQF, double quantum filtered; TPPI, time proportional phase increments; COSY, (scalar) correlation spectroscopy; RECSY, relayed correlation spectroscopy; TOCSY, total correlation spectroscopy; NOESY, nuclear Overhauser effect (dipolar correlation) spectroscopy; HSQC, heteronuclear single quantum correlation.

[2] We will use the terms "extractable" or "free" to distinguish the GIPC structures discussed herein from the GIPC lipid anchors found covalently linked to surface membrane glycoproteins in *Saccharomyces cerevisiae* (*1*), whose structures are known in considerable detail (*2*) (see Discussion).

S0006-2960(97)03008-0 CCC: $15.00
Published on Web 05/29/1998

characterized GIPC antigens of *H. capsulatum* (*14*, *15*), very few structures of free GIPC are known in detail; for example, to date only compositional analysis data have been published for the GIPCs of *A. niger* (*16*, *17*). A complex composite structure was reported for GIPCs from *Agaricus bisporus* (*4*), but the experimental evidence for it has not yet been published. Although the broadly distributed α-mannosyl-*myo*-inositol-phosphorylceramide (MIPC) was initially characterized over thirty years ago (*18*, *19*), and a claim for the structure Manα1→2Ins1-P-1Cer made (*4*), to our knowledge no data unequivocally establishing the precise linkage position of the Man residue on the Ins ring have been published.

In this paper we describe the structure elucidation of two GIPCs extracted from *Paracoccidioides brasiliensis*, a mycopathogen endemic to rural areas of South and Central America (*20*, *21*). Like *H. capsulatum*, *P. brasiliensis* is a thermally dimorphic fungus, growing in yeast form at 37 °C, and in mycelium form at 23 °C (*22*, *23*). Infection by *P. brasiliensis* is prevalent among farm workers, commonly affecting the lungs, lymphoid, and mucocutaneous tissues; in severe cases a deep mycosis may involve bone or spinal cord (*24*−*27*). One of the GIPCs from *P. brasiliensis*, called Band 1 (referred to herein as Pb-**1**), was found to be reactive with the sera of all patients exhibiting paracoccidioidomycosis (PCM), but not with sera of healthy donors or patients with histoplasmosis (*28*). The second GIPC, called Band 2 (referred to herein as Pb-**2**), was not reactive with PCM sera. It has been proposed (*28*, *29*) that an immunodominant β-galactofuranose is present as a nonreducing terminal residue in the glycan of Pb-**1**. Other structural features, including the nature of the lipid moiety, have not been well characterized. We now report the complete structure elucidation of *P. brasiliensis* glycosphingolipids Pb-**1** and Pb-**2** with respect to both their glycan and ceramide moieties; in particular, all glycosyl linkages have now been determined unambiguously, including that of the β-galactofuranose residue. The addition of Manα1→2 to *myo*-inositol as a key step in the glycosylation of IPC has also been confirmed for this fungus. This information suggests a number of common features of fungal GIPC biosynthesis, some of which might represent potential targets for diagnosis and therapy of fungal disease.

MATERIALS AND METHODS

Glycosylinositol Phospholipids. Glycolipids were extracted from mycelium and yeast forms of *P. brasiliensis* and purified by DEAE-Sephadex chromatography, HPLC, and HPTLC as described previously (*28*−*30*). Two major glycolipids, Pb-**1** and Pb-**2**, were isolated from the acidic fractions eluted from DEAE-Sephadex by 0.2 M sodium acetate in MeOH. Compound Pb-**1**, having the lower R_f value on HPTLC analysis, was the major acidic glycolipid found in the yeast form, making up about 90−95% of the acidic fraction; compound Pb-**2** could be isolated in significant quantities only from the mycelium form, where it comprised about 40−45% of the acidic fraction (*28*).

Release of Glycosylinositols by Ammonolysis. Ammonolysis of *P. brasiliensis* glycolipids was performed essentially as described by Barr and Lester (*14*), with some variation in the workup procedure. Briefly, aliquots of lipid (100−300 μg) were heated in a tightly sealed Teflon-lined screw-capped test tube with 10 N NH_3•H_2O (1−2 mL) for 18 h at 150 °C. After cooling, the solution was evaporated to dryness under N_2 stream at 40 °C; this was repeated after addition of a few drops of 2-propanol. The residue was taken up in 1 mL H_2O, and after thorough sonication lipophilic components were removed by passage of this solution through a small C18-silica solid-phase extraction cartridge, washing with 2 × 1 mL H_2O. The combined aqueous solution containing free glycosylinositol and an equivalent amount of phosphate was lyophilized and used without further purification; the small amount of salt present did not appear to interfere significantly in subsequent analytical procedures. The glycosylinositols are referred to as GI-**1** and -**2**). The lipophilic components were eluted from the C18-silica cartridge with MeOH (3 mL) and $CHCl_3$-MeOH (1:1 v/v; 2 mL), and evaporated to dryness under N_2 stream at 40 °C.

^{1}H and ^{31}P Nuclear Magnetic Resonance Spectroscopy. ^{1}H NMR spectroscopy was performed at 500 or 600 MHz with Bruker AM-500 (University of Washington), AMX-500, or DRX-600 (University of Georgia/Complex Carbohydrate Research Center) spectrometers. ^{31}P NMR spectroscopy was performed at 202.4 MHz on the AMX-500 spectrometer. ^{1}H-detected ^{31}P-^{1}H heteronuclear correlation spectra were acquired on the AMX-500 spectrometer using a 1-D version of the experiment described by Bax et al. (*31*). For NMR experiments, samples of native *P. brasiliensis* glycolipids Pb-**1** and -**2** (1−1.5 mg) were deuterium exchanged by repeated addition and evaporation of $CDCl_3$/CD_3-OD 1:1, and dissolved in 0.5 mL DMSO-d_6/D_2O 98:2 (*32*). All experiments in this solvent were carried out at 308 K. Samples of free glycosylinositols released by ammonolysis (GI-**1** and -**2**) were deuterium exchanged by repeated lyophilization from D_2O, and dissolved in 0.5 mL of D_2O. All experiments in D_2O were carried out at 298 °K. In all proton NMR experiments, suppression of the residual HOD resonance was accomplished by a presaturation pulse during the preparatory delay period (PD = 2.0 s). For 1-D spectra, the sweep width was 10 ppm, collected over 16K data points.

Pure absorption PS−COSY with double quantum filtering (DQF) (*33*, *34*), TOCSY (*35*) using the MLEV-17 pulse scheme described by Bax and Davis (*36*) (120, 180, and 240 ms mixing times), and homonuclear PS−NOESY spectra (300 ms mixing time) were all recorded using the method of time proportional phase increments (TPPI) (*37*, *38*), with parameters for acquisition and processing essentially as described previously (*39*). One-step relayed coherence transfer (RECSY or RELAY) (*40*) spectra were acquired and transformed as described (*39*), but with a mixing time of 100 ms, optimal for $^3J_{x,y} + {}^3J_{y,z} = 10$ Hz (*41*), a compromise value for the expected combined couplings. A total of 512 t_1 experiments were collected, with a sweep width of 6000 Hz collected over 4K data points in t_2; an increment to t_2 of 0.166 ms gave a $t_{2max} = 85$ ms.

Monosaccharide, Fatty Acid, Inositol, and Linkage Analysis. Methanolysis (1.0 mL 1 N HCl in anhydrous MeOH at 80 °C for 16−22 h), re-*N*-acetylation (200 μL MeOH, 40 μL pyridine, 40 μL acetic anhydride for 30 min at room temperature), and per-*O*-trimethylsilylation of the resultant monosaccharide methyl glycosides [200 μL Tri-Sil (Pierce,

Rockford, IL) at 80 °C for 30 min] were performed on ca. 50 μg samples of dry GIPC essentially as described by Merkle and Poppe (*42*), except that fatty acid methyl esters (FAMEs) were extracted from the cooled methanolysate by partitioning with an equal volume of hexane (3×) prior to drying under N_2 at 40 °C. The combined hexane extracts were also dried carefully under N_2 at 40 °C, and per-*O*-trimethylsilylated with Tri-Sil using an identical protocol [after cooling the reactants to room temperature, the Tri-Sil reagent was removed by careful drying under N_2 at 40 °C, and the residue extracted with *n*-hexane (2 × 100 μL)] for GC-MS analysis. Sphingosines were released using conditions described by Gaver and Sweeley (1965), washed with hexane and dried, *N*-acetylated with pyridine and acetic anhydride in methanol, and per-*O*-trimethylsilylated for GC-MS analysis with Tri-Sil as described above. Lengthy protocols (*43*, *44*) for isolating sphingosines from the methanolysate prior to derivatization were omitted, since all of the per-*O*-trimethylsilylated monosaccharide derivatives eluted well before those of the sphingosines, and did not interfere in their detection. Inositols were released and peracetylated for GC-MS analysis as described by Barr and Lester (*14*).

All GC-MS analyses were performed on a Hewlett-Packard 5890 GC/5970 MSD using splitless injection. Analysis of inositol per-*O*-acetates was performed on a 50 m Quadrex methylsilicone bonded phase fused silica capillary column, temperature programmed from 170 to 320 °C at 3°/min. All other component analyses were performed on a 30 m DB-5 bonded phase fused silica capillary column, temperature programmed from 160 to 200 °C at 2°/min and from 200 to 260 °C at 10°/min (for per-*O*-TMS methyl glycosides); or from 140 to 320 °C at 4°/min (for FAMEs and *N*-acetyl, per-*O*-TMS sphingosines). All derivatives were identified by retention times and mass spectra compared with authentic standards and published data.

Permethylation, hydrolysis, reduction, and acetylation to produce PMAAs were performed as described by Levery and Hakomori (*45*). PMAAs were analyzed on the DB-5 column and the GC-MS system described above, temperature programmed from 160 to 260 °C at 2°/min, with derivatives identified by retention times and characteristic EI mass spectra (*46*, *47*) compared with those of authentic standards.

Positive Ion Electrospray Mass Spectrometry. ESI-MS experiments were performed on a PE-Sciex API-III spectrometer with IonSpray source. Samples were dissolved in methanol containing 1 mM ammonium acetate, and introduced by direct infusion. For single quadrupole scanning, the mass range of *m*/*z* 100−1600 was scanned at an orifice potential of 180 V. For tandem MS-CID-MS experiments, argon was introduced into the collision cell at a CGT ≅ 350−400, precursor ions were selected in Q_1 while an appropriate mass range was scanned in Q_3. The potential difference across the collision cell was set ≅80 V. Fragment nomenclature is according to Costello and Vath (*48*). However, it should be noted that the structure of the sodiated B_i fragments are not identical to those of B_i fragments produced by high-energy FAB-MS/CID-MS processes. The designation B_i has been assigned (*48*) to oxonium ions formerly referred to as A-type (*49*); in ESI-MS/CID-MS of sodium adducts, the analogous fragment is essentially the other product of Y-type cleavage (*48*), formerly called β-cleavage (*49*), which is only detectable if it retains a cation, as is the case in positive ion mode ESI-MS.

α-*Mannosidase Treatment of the Glycosylinositol Released from Glycolipid Pb-**2** by Ammonolysis.*To an aliquot of GI-**2** (ca. 35 μg) in 70 μL H_2O was added an equal volume of 0.1 M sodium acetate buffer (pH adjusted to 4.5 with HAc), followed by 60 μL Jack Bean α-mannosidase (Boehringer-Mannheim, 5 mg/mL suspension). The reaction mixture was sealed and agitated gently for 3 h at 37 °C. A second portion of α-mannosidase (50 μL) was added, and incubation was continued for 16 h more. The reaction mixture was then transferred to a larger vessel, washing with 2 × 1 mL H_2O, and lyophilized. The mixture was then lyophilized twice more from 1.4 mL D_2O, and dissolved in 0.5 mL D_2O for NMR spectroscopy. As controls, small amounts of pure mannose and *myo*-inositol (ca. 0.1−0.3 mg) were treated in identical fashion except that the incubation period was omitted. Following acquisition of 1-D ^1H NMR spectra, the three samples were recovered, lyophilized, and redissolved in H_2O (1 mL).

Each sample was then treated as follows for GC-MS analysis of sugars as per-*O*-acetylated alditol and inositol derivatives. Reduction was carried out by addition of 1.0 mL $NaBH_4$ solution (10 mg/mL in 0.01 N NaOH); after thorough vortexing, the solutions were allowed to stand overnight at 4 °C. After addition of a few drops of HAc to destroy the remaining borohydride, the reaction mixture was evaporated to dryness under N_2 stream at 40 °C, with addition of EtOH to azeotrope the H_2O. The residue was then freed of borate by 5× addition of 5% HAc in MeOH (1 mL) and evaporation to dryness under N_2 stream at 40 °C. The remaining residue was dried in vacuo over NaOH and per-*O*-acetylated by heating with acetic anhydride (1 mL) in a sealed tube for 2 h at 100 °C. After cooling and evaporating just to the point of dryness under N_2 stream, with addition of toluene to azeotrope the acetic anhydride, the per-*O*-acetylated sugars were recovered for GC-MS by partitioning the residue between $CHCl_3$ and H_2O (1 mL each), washing the $CHCl_3$ layer several times with additional H_2O. The $CHCl_3$ layer was then carefully evaporated to dryness and the sugar acetates taken up in fresh $CHCl_3$ for GC-MS analysis.

RESULTS

*Monosaccharide, Sphingosine, Fatty Acid, and Inositol Component Analysis of Purified Glycolipid Fractions Pb-**1** and Pb-**2**.* Following methanolysis of glycolipid fractions Pb-**1** and Pb-**2**, GC-MS analysis of monosaccharides as their TMS methyl glycosides showed Pb-**1** to consist of mannose and galactose in a ratio of 2.00:1.17, while Pb-**2** yielded only mannose as a significant component. Small amounts of glucose were detected in both glycolipid fractions, along with a small amount of galactose in glycolipid fraction **2**, but subsequent NMR and MS analysis confirmed that these were not derived from the major components of each fraction (*vide infra*).

When the methanolysates were re-*N*-acetylated prior to trimethylsilylation, no peaks corresponding to hexosamine derivatives were observed; however, a small very late eluting peak (40.9 min) was detected in each chromatogram; the EI mass spectrum of this component was similar in appearance

to that of *N*-acetyl-1,3,4-tri-*O*-trimethylsilyl-(t18:0)-4-hydroxysphinganine (= phytosphingosine) published previously (*50*), except that we observed additional peaks corresponding to $M^{\bullet+}$, $[M-15]^+$, and $[M-15-90]^+$ (*m/z* 575, 560, and 470, respectively), confirming the molecular mass of the derivative. The GC retention time and EI mass spectrum were identical to those of authentic *N*-acetyl-1,3,4-tri-*O*-trimethylsilyl-(t18:0)-4-hydroxysphinganine analyzed under the same conditions, and distinct from those of both *N*-acetyl-di-*O*-trimethylsilyl-(d18:1)-sphing-4-enine and *N*-acetyl-di-*O*-trimethylsilyl-(d18:0)-sphinganine. When the modified methanolysis reagent of Gaver and Sweeley (*44*) was used, the yield of this derivative increased approximately 5-fold, to about half of the total response of per-*O*-trimethylsilyl mannose derivatives.

When GC-MS analysis of the hexane extracts following methanolysis was performed, only small amounts of 16:0 and 18:0 fatty acids were detected as their methyl esters. After *O*-trimethylsilylation of the extracts, abundant peaks for the trimethylsilyl derivatives of 2-hydroxy-fatty acid methyl esters were observed. Both glycolipids Pb-**1** and -**2** had h24:0 fatty acid as the major component, with smaller amounts of h18:0, h20:0, h22:0, h23:0, and h25:0 also detected.

Following strong acid hydrolysis and peracetylation, an additional component was detected from both glycolipids by GC-MS, identical in GC retention time and EI mass spectrum to an authentic standard of hexa-*O*-acetyl-*myo*-inositol. The retention time of this derivative was distinct from those of *epi*- and *scyllo*-inositols analyzed under the same conditions.

In summary, glycolipid Pb-**1** was found to consist of mannose and galactose in a ratio of 2:1, along with *myo*-inositol and a ceramide consisting primarily of t18:0 phytosphingosine and h24:0 fatty acid. The presence of one or more phosphate moieties was assumed on the basis of positive staining with Dittmer-Lester reagent (*50*). Glycolipid Pb-**2** appeared to be similar in all respects, except that it lacked the galactose residue.

*1- and 2-D ^{1}H NMR Spectroscopy of Glycolipid Pb-**2**.* In Figure 1A is reproduced a downfield expansion (2.8−5.1 ppm) of the 1-D ^{1}H NMR spectrum of glycolipid Pb-**2** in DMSO-d_6/2% D_2O. As expected for a glycosphingolipid having a fully saturated ceramide moiety, virtually no resonances for either cis or trans-vinyl protons were detected (5.3−5.6 ppm; not shown). Characteristic resonances for long-chain acyl bulk CH_2 and terminal CH_3 protons were observed at 1.23 and 0.85 ppm, respectively (not shown). Two anomeric resonances were observed at 5.061 and 4.896 ppm, both having $^3J_{1,2}$ on the order of their apparent line widths (≤ 2 Hz); the resolution was judged insufficient for unambiguous determination of the anomeric configuration of Man residues.

Use of 2-D proton scalar correlation experiments, including PS-DQF−COSY (Figure 2A) and TOCSY (available as Supporting Information), facilitated nearly complete unambiguous assignment of sugar ring and exocyclic proton resonances starting from the two anomeric signals. Approximate ring proton $^3J_{i,j}$ coupling constants were consistent with *manno*pyranosyl spin systems. In addition, a cyclic six-membered spin system was clearly delineated, with a set of $^3J_{i,j}$ coupling constants consistent with *myo*-inositol, having a lone equatorial ring proton, H-2 ($^3J_{1,2}$ and $^3J_{2,3}$ were small

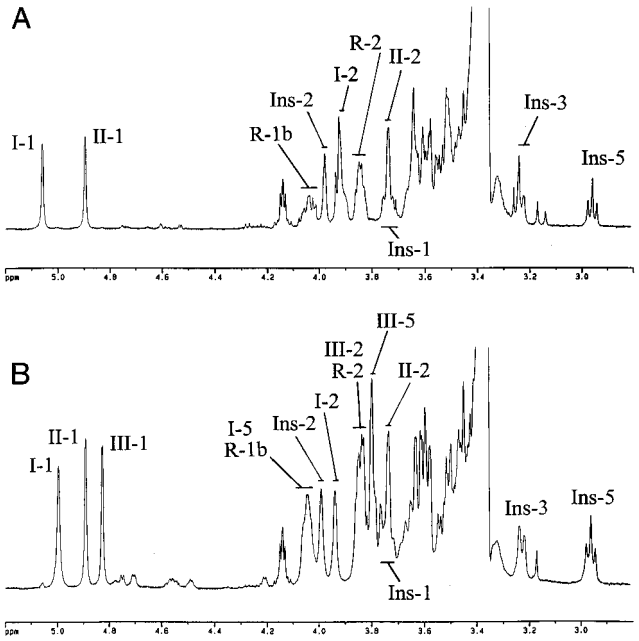

FIGURE 1: Downfield expansion of 1-D proton NMR spectra of P. brasiliensis glycolipids Pb-**2** (Panel A) and Pb-**1** (Panel B) in DMSO-d_6/D_2O 98:2 at 308 K. Arabic numerals refer to ring protons of residues designated by Roman numerals or capital letters in the corresponding structure drawn at the top of Table 1. R refers to proton of the sphingosine backbone only. Ins = *myo*-inositol.

[ax/eq and eq/ax], while the remaining $^3J_{i,j}$ were large [ax/ax]). Of the two direct coupling partners of H-2, at 3.220 and 3.730 ppm, the latter appeared to exhibit an additional splitting besides those to its nearest neighbors (Figure 2A); this was taken as evidence of coupling to a ^{31}P nucleus, and that proton tentatively assigned as H-1 of *myo*-inositol. The proton resonance assignments for the monosaccharide and *myo*-inositol (Ins) ring spin systems are summarized in Table 1.

An additional spin system, beginning with a pair of proton resonances at 3.642 and 4.028 ppm and terminating in the bulk acyl CH_2 signal, was assigned to the phytosphingosine chain of the ceramide moiety (column R, Table 1).

In a 2-D proton dipolar correlation spectrum (NOESY; available as Supporting Information) acquired with a mixing time of 300 ms, two strong correlations were observed from the H-1 resonating at 5.061 ppm; these corresponded to an intraresidue dipolar correlation with H-2, as expected for either an α- or *β*-Man*p* residue; and an *inter*residue dipolar coupling of comparable intensity with H-2 of the *myo*-inositol residue, taken as compelling evidence for a Man*p*1→2Ins linkage. From the other H-1, resonating at 4.896 ppm, an intraresidue correlation was again observed with the vicinal H-2; in addition, a strong interglycosidic correlation was observed with Man*p* I-3, as well as weak ones with I-2 and I-4, which were taken together as evidence for a Man*p*1→3Man linkage. The dipolar correlation data are summarized in Table 2.

*1-D ^{31}P NMR Spectroscopy of Glycolipid Pb-**2**.* In a 1-D proton-decoupled ^{31}P NMR spectrum of glycolipid Pb-**2** (not shown), a single resonance was observed 4.33 ppm downfield from an external H_3PO_4 standard. A 1-D ^{31}P-filtered ^{1}H NMR spectrum (available as Supporting Information) showed three proton correlations for this phosphorus nucleus; one with the resonance assigned as Ins-1 (3.730 ppm), and with

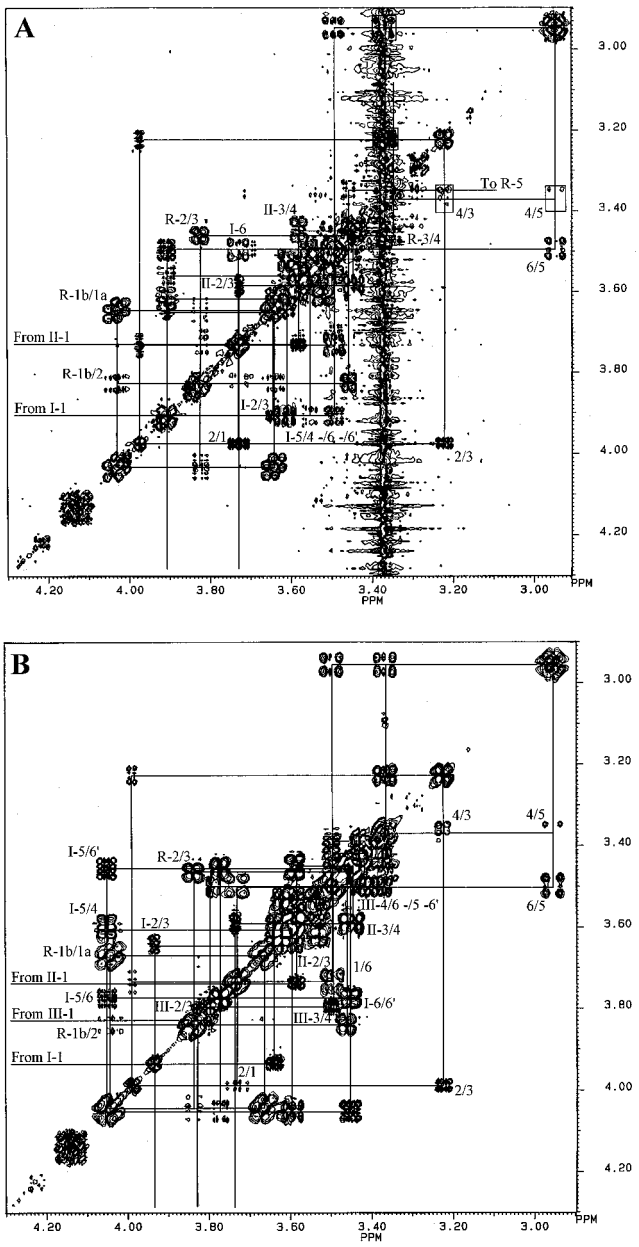

FIGURE 2: Downfield regions of 2-D PS-DQF-COSY spectra of *P. brasiliensis* glycolipids Pb-**2** (Panel A) and Pb-**1** (Panel B) in DMSO-d_6/D_2O 98:2 at 308 K.

the pair of resonances assigned as R-1a and −1b of the ceramide moiety (3.642 and 4.028 ppm, respectively). The correlations confirmed those assignments, and enabled a preliminary proposal for the structure of glycolipid Pb-**2**, Man*p*1→3Man*p*1→2Ins(1-*O*-Phosphoryl→1)Cer, complete except for the anomeric configurations of the Man*p* residues.

*1- and 2-D ^{1}H NMR Spectroscopy of Glycosylinositol Released from Glycolipid Pb-**2** by Ammonolysis.* NMR spectroscopy was performed on the glycosylinositol released from glycolipid Pb-**2** (GI-**2**) with the expectation that high-resolution spectra in D_2O, free from the influence of the phosphate group, would allow correlation with the extensive database now available for oligomannose structures, and thus provide a clear indication of the anomeric configurations of the two Man*p* residues in this compound. In the 1-D spectrum (Figure 3A), two anomeric resonances were observed at 5.150 and 5.127 ppm, well in the region expected for α-Man*p* residues. Furthermore, $^3J_{1,2}$ coupling constants

Table 1: Chemical Shifts (ppm) for Ceramide, Inositol, and Monosaccharide Ring Protons of *P. brasiliensis* Glycosphingolipid Antigens in DMSO-d_6/D_2O 98:2 at 308 K[a]

	residue				
	III	II	I	inositol	R
	Gal*f*β1⟶6				
			Man*p*α1⟶2Ins1← P →1Ceramide		
proton		Man*p*α1⟶3			
H-1		4.896	5.061	3.730	3.642, 4.028
H-2		3.728	3.910	3.970	3.839
H-3		3.580	3.647	3.220	3.459
H-4		3.446	3.609	3.370	3.347
H-5		*3.580*	3.905	2.950	
H-6		*3.610*	3.558	3.492	
H-6′		*3.518*	3.492		
H-1	4.825	4.886	4.995	3.730	3.661, 4.039
H-2	3.827	3.733	3.932	3.986	3.833
H-3	3.794	3.587	3.638	3.220	3.456
H-4	3.494	3.448	3.595	3.362	3.354
H-5	*3.396*	*3.587*	4.050	2.950	
H-6	*3.427*	*3.617*	3.771	3.493	
H-6′	*3.369*	*3.524*	3.452		

[a] Tentative assignments in italics. Numbering of *myo*-inositol ring protons differs from that in ref *29*.

Table 2: Summary of Dipolar Correlations Observed from H-1 of Hex Residues in NOESY Spectra of *P. brasiliensis* Glycosphingolipid Antigens Pb-2 and Pb-1[a]

		dipolar correlation		
antigen	origin	strong	medium	weak
Pb-**2**	***II-1*→**	***I-3***	I-2	
		II-2	I-4	
	***I-1*→**	***Ins-2***		
		I-2		
Pb-**1**	***III-1*→**		***I-6***	***I-6′***
			III-2	
			III-3	
	***II-1*→**	***I-3***	I-2	II-3/I-4
		II-2	I-4	
	***I-1*→**	***Ins-2***		I-3
		I-2		I-4
				I-5

[a] Key interresidue correlations indicated by boldface italics.

could be measured more easily under these conditions, and their values, 1.46 and 1.84 Hz, respectively, were both clearly within the limits observed for the α-configuration of mannosyl residues. Typical values for the chemical shift and $^3J_{1,2}$ of β-Man*p* are around 4.7−4.8 ppm and 0.9 Hz, respectively. A 2-D correlation experiment (Figure 3B) allowed assignment of the corresponding Man*p* H-2 resonances (4.076 and 4.240 ppm, respectively); from these the values of $^3J_{1,2}$ could be confirmed and $^3J_{2,3}$ coupling constants also measured. The appearance of the H-2 resonances corresponded to those descibed by Vliegenthart et al. (*51*) as characteristic for α-Man*p* residues. Finally, comparison with several database entries for structures containing a nonreducing terminal Man*p*α1→3Man*p*α1→2Man*p* fragment showed typical chemical shift values of 5.143 and 4.060 ppm for H-1 and H-2, respectively, of the terminal residue (*52*), comparable with the 5.150 and 4.076 ppm pair observed for GI-**2**. Values given for H-1 and H-2 of the internal residue of the trimannose fragment were 5.038 and 4.224 ppm, respectively (*52*); compared with the chemical shifts 5.127 and 4.240 ppm observed for the same protons in the second Man*p* residue of GI-**2**, the values for H-2 appeared to be

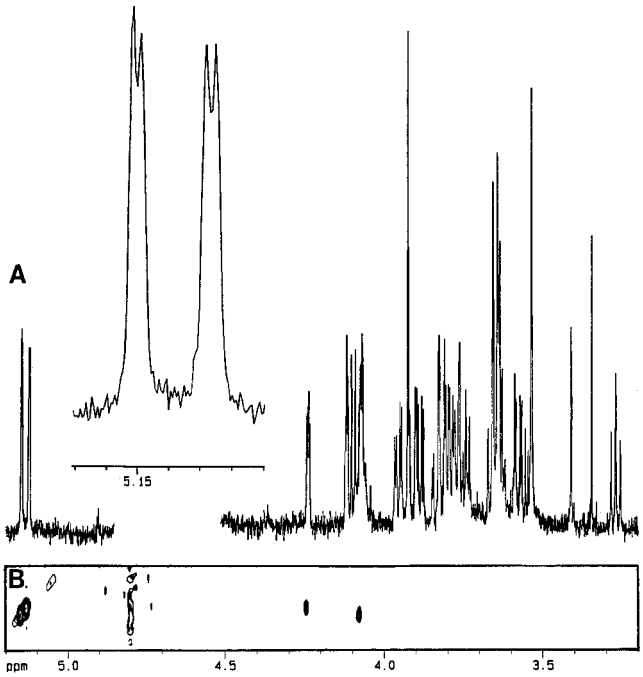

FIGURE 3: Downfield expansions of 1- and 2-D proton NMR spectra of *P. brasiliensis* glycosylinositol GI-**2** in D_2O at 298 K. Panel A, 1-D proton spectrum; Inset, expansion of anomeric proton region. Panel B, section of 2-D TOCSY spectrum showing H-1/H-2 scalar correlations.

Table 3: Chemical Shifts (ppm) and Coupling Constants (Hz), in D_2O at 298 K, for Selected Monosaccharide Ring Protons of *P. brasiliensis* Glycosylinositols (X = Ins) Compared with Data for the Terminal Disaccharide Fragment of a Glycan Released from a Secreted Glycoprotein of *S. cerevisiae* [X = α-Man (*52*)]

	residue			
	III	II	I	
	Gal*f*β1⟶	⟶6		
			Man*p*α1⟶	⟶2X
proton		Man*p*α1⟶3		
H-1		5.143	5.038	X = α-Man
H-2		4.060	4.224	
H-1		5.150	5.127	X = Ins
$^3J_{1,2}$		(1.46)	(1.84)	
H-2		4.076	4.240	
$^3J_{2,3}$		(3.30)	(3.30)	
H-1	5.041	5.151	5.091	X = Ins
$^3J_{1,2}$	(1.99)	(1.49)	(1.74)	

close, while those for H-1 exhibited a wider variance. However, this is not unexpected in view of the difference in the aglycone between the two structures. These data, summarized in Table 3, clearly support the structure of GI-**2** as Man*p*α1→3Man*p*α1→2Ins (Scheme 1, R = H).

*1- and 2-D ^{1}H NMR Spectroscopy of Glycolipid Pb-**1**.* In Figure 1B is reproduced a downfield expansion (2.8−5.1 ppm) of the 1-D ^{1}H NMR spectrum of glycolipid Pb-**1** in DMSO-d_6/2% D_2O. In this case, three anomeric resonances were observed at 4.995, 4.886, and 4.825 ppm, all with $^3J_{1,2}$ on the order of their apparent line widths (≤2 Hz). As with glycolipid Pb-**2**, 2-D proton scalar correlation experiments on glycolipid Pb-**1** enabled nearly complete unambiguous assignment of the sugar ring and exocyclic proton resonances starting from the three anomeric signals, as well as identification of similar *myo*-inositol and phytosphingosine spin

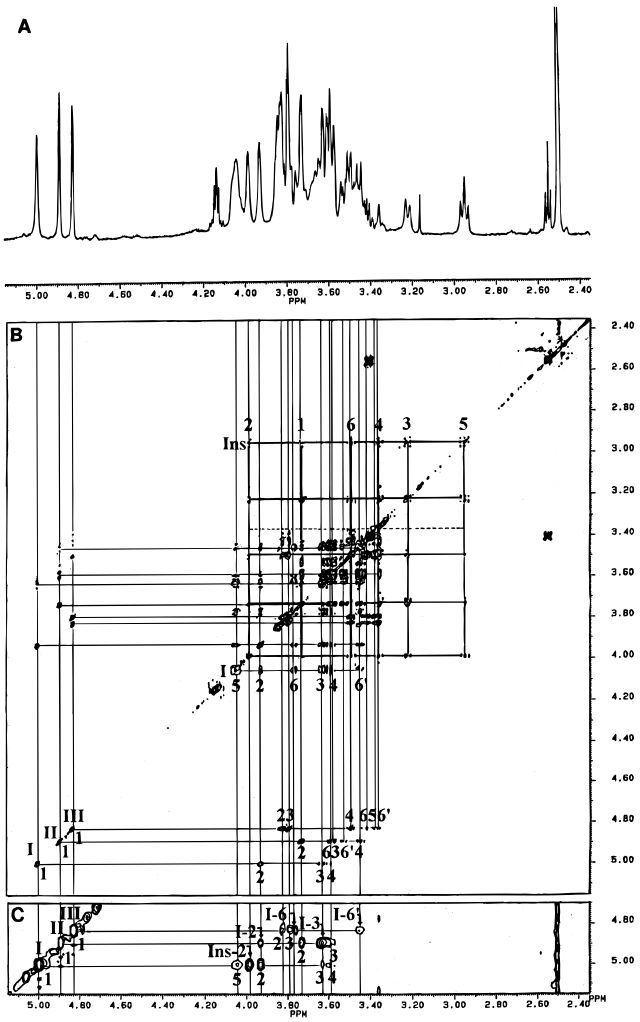

FIGURE 4: Downfield regions of 1-D proton NMR spectrum (Panel A), along with 2-D TOCSY (Panel B) and NOESY (Panel C) spectra of Pb-**1** in DMSO-d6/D2O 98:2 at 308 K.

systems (Figure 2B; Figure 4A,B). The proton chemical shift assignments are summarized in Table 1. Approximate ring proton $^3J_{i,j}$ coupling constants were consistent with two *manno*pyranosyl spin systems, again having unspecified anomeric configurations, arising from the H-1 signals at 4.995 and 4.886 ppm; and a *β-galacto*furanosyl spin system arising from the H-1 at 4.825 ppm. In the latter case, the small $^3J_{1,2}$ would appear to rule out α-Gal*f*, since the smaller H-1/H-2 dihedral angle would be expected to yield a larger coupling constant [$^3J_{1,2}$ for methyl α-galactofuranoside has been measured at 4.0 Hz; for methyl *β*-galactofuranoside, 2.0 Hz (*53*, *54*)].

A 2-D NOESY experiment on glycolipid Pb-**1** (Figure 4C, Table 2) again allowed the linkage structure to be deduced. As before, a strong interglycosidic correlation was observed from H-1 of one of the Man*p* spin systems (I-1; 4.995 ppm) to H-2 of the *myo*-inositol residue, accompanied by a strong intraresidue dipolar coupling to the vicinal H-2 and weaker couplings to H-3, H-4, and H-5. In light of the evidence presented for the structure of glycolipid Pb-**2**, as well as additional data obtained for glycolipid Pb-**1** (*vide supra*), we interpret the weak H-1/H-5 dipolar correlation as a transferred NOE, arising through rapid spin diffusion via H-2/H-3/H-4, rather than implying an axial (*β*-anomeric) configuration for H-1. This may be due to an increase in the

Scheme 1: Structure of Pb-**2** (R = Cer-P-) and GI-**2** (R = H)

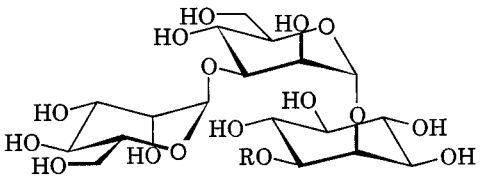

Scheme 2: Structure of Pb-**1** (R = Cer-P-) and GI-**1** (R= H)

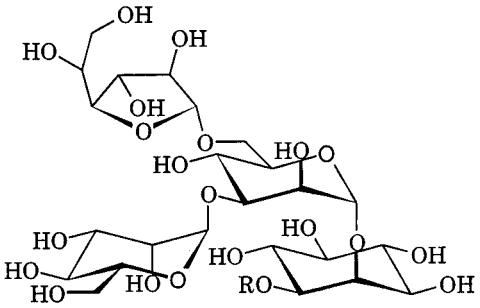

correlation time for this residue, relative to that in glycolipid Pb-**2**, as a consequence of the additional sugar linked to it.

As with glycolipid Pb-**2**, an intense interglycosidic correlation was observed between H-1 of the second Man*p* residue (II-1; 4.886 ppm) and H-3 of the first, accompanied by a strong intraresidue correlation with the vicinal II-2 and weaker correlations with I-2 and I-4/II-3. Assuming, as will be shown further, that these residues are configured as they are in glycolipid Pb-**2**, the partial structure Man*p*α1→3-Man*p*α1→2Ins can be proposed. Finally, from the third anomeric signal, assigned as H-1 of *β*-Gal*f* (III-1; 4.825 ppm), intraresidue dipolar correlations were observed to III-2 and III-3, accompanied by a strong correlation with I-6 and a weak one with I-6′, consistent with a Gal*fβ*1→6 linkage to the internal Man residue. The complete structure for the glycan of glycolipid Pb-**1** can therefore be proposed as Gal*fβ*1→6(Man*p*α1→3)Man*p*α1→2Ins (Scheme 2, R = H).

*1-D ^{31}P NMR Spectroscopy of Glycolipid Pb-**1**.* In a 1-D proton decoupled ^{31}P NMR spectrum of glycolipid Pb-**1**, a single resonance was observed 3.87 ppm downfield from an external H_3PO_4 standard. A 1-D ^{31}P-filtered ^{1}H NMR spectrum (available as Supporting Information) again showed three proton correlations for this phosphorus nucleus; one with the resonance assigned as Ins-1 (3.730 ppm); and with the pair of resonances assigned as R-1a and −1b of the ceramide moiety (3.661 and 4.039 ppm, respectively). The correlations confirmed those assignments, as well as the complete structure of glycolipid Pb-**1**, Gal*fβ*1→6(Man*p*α1→3)-Man*p*α1→2Ins(1-*O*-Phosphoryl→1)Cer (Scheme 2, R = Cer).

*1-D ^{1}H NMR Spectroscopy of Glycosylinositol Released from Glycolipid Pb-**1** by Ammonolysis.* A 1-D proton NMR spectrum (not shown), taken in D_2O, of the glycosylinositol released from glycolipid Pb-**1** (GI-**1**) exhibited three anomeric proton resonances, at 5.151, 5.091, and 5.041 ppm. By analogy with the spectrum of GI-**2**, and taking into account the chemical shift differences observed for the H-1 resonances on going from glycolipid Pb-**2** to glycolipid Pb-**1** in DMSO-d_6 (Man*p* II-1 relatively unchanged; Man*p* I-1 shifted upfield; Gal*f* III-1 resonating furthest upfield), these were assigned as Man*p* II-1, Man*p* I-1, and Gal*f* III-1, respectively. As was the case for GI-**2**, both the chemical shifts and the $^3J_{1,2}$ coupling constants (Table 3) in this medium clearly support the α-configurations for both of the Man*p* residues in GI-**1**.

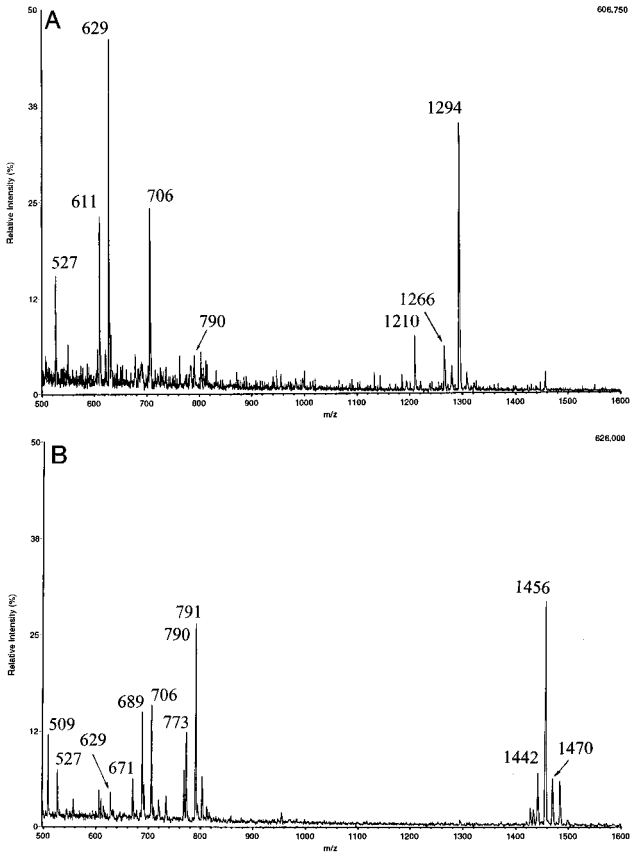

FIGURE 5: Positive ion mode ESI-CID-MS of glycolipids Pb-**2** (Panel A) and Pb-**1** (Panel B).

Electrospray Ionization Mass Spectrometry. A number of techniques were employed to ensure a high confidence level for the proposed structures. Analysis of the native purified glycolipids by ESI-MS provided independent confirmation of a number of structural features, including the glycan size and sequence, the position of the phosphate group, and the ceramide profile. In the positive ion mode, singly charged pseudomolecular ions $[M-H+2Na]^+$ of both glycosylinositol phospholipids were readily observed (Figure 5A, B) at *m*/*z* ratios differing by 162 u, corresponding to the mass of a single hexose residue. Detection of singly charged species was found to be optimal at high orifice-to-skimmer potentials (180 V was used for all experiments described). Under these conditions, a number of useful fragment ions were also detected in high abundance between *m*/*z* 500−800. However, the presence of other ions not clearly assignable, along with increasingly abundant background noise below *m*/*z* 500, prompted the use of ESI-MS/MS studies for more detailed structural interpretations.

In each case, product ion spectra were recorded while selecting the major pseudomolecular ion (Figure 6A,B), as well as fragments corresponding to the phosphorylated glycans, $[C_3PO_3Na_2]^+$ and $[B_3PO_3Na_2]^+$ (Figure 7A,B for Pb-**1**; spectra for Pb-**2** included in Supporting Information). Interpretations of the resultant product ions, with respect to

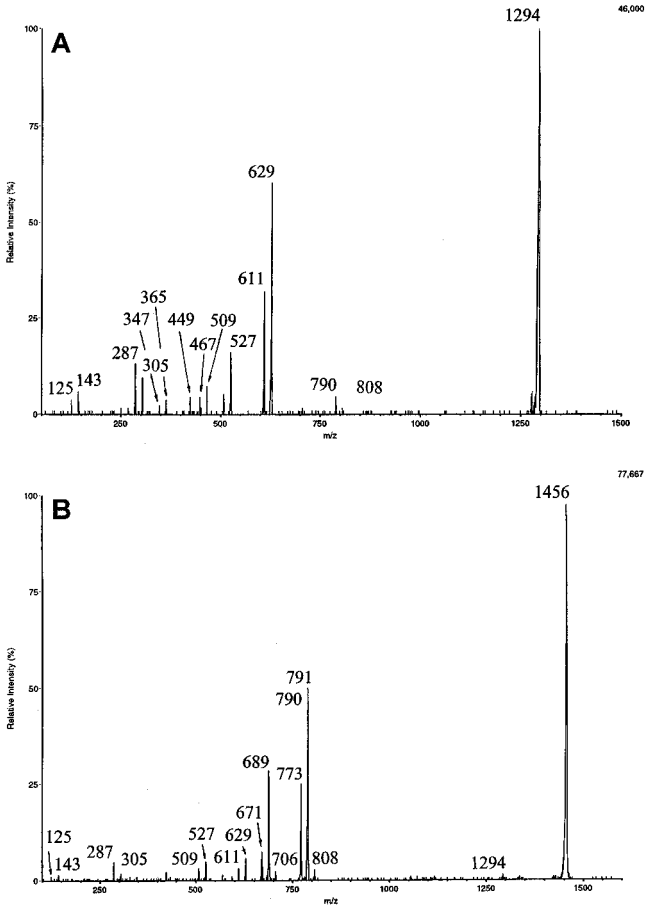

FIGURE 6: Product ion spectra from ESI-CID-MS/CID-MS experiments on glycolipids Pb-**2** (Panel A) and Pb-**1** (Panel B). Selected precursors: Panel A, *m*/*z* 1294 (major pseudomolecular ion of glycolipid Pb-**2**; Panel B, *m*/*z* 1456 (major pseudomolecular ion of glycolipid Pb-**1**. Fragments are interpreted according to Schemes 3 and 4 and Table 4.

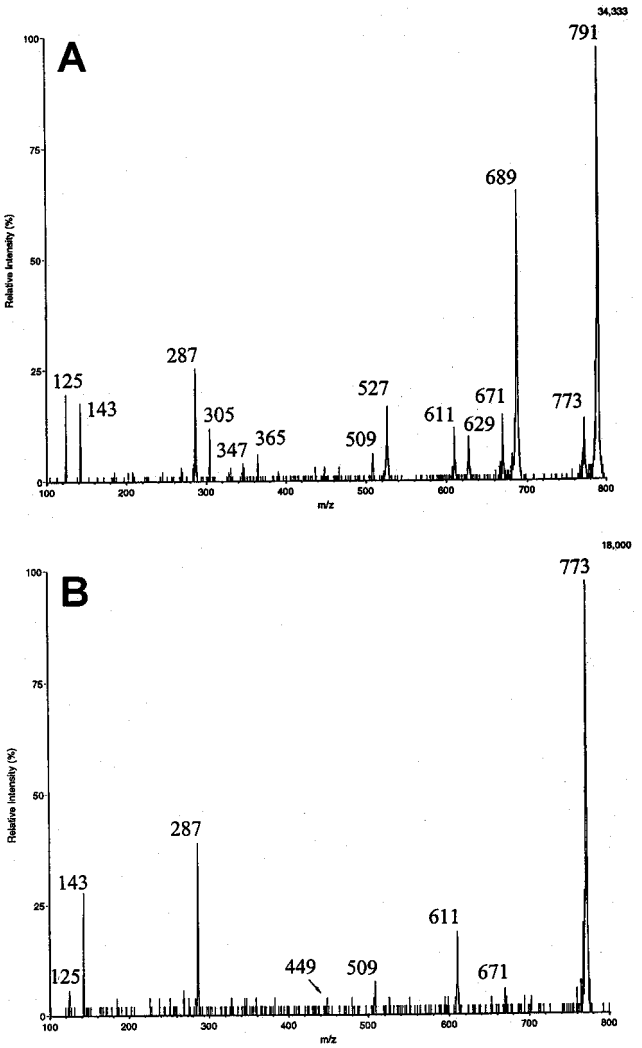

FIGURE 7: Product ion spectra from ESI-CID-MS/CID-MS experiments on glycolipid Pb-**1**. Selected precursors: Panel A, *m*/*z* 791 (C_3PO_3Na); Panel B, *m*/*z* 773 (B_3PO_3Na). Fragments are interpreted according to Scheme 4 and Table 4.

known low-energy CID behavior of glycoconjugates, are summarized in Schemes 3 and 4 and Table 4. Of particular relevance is the extremely low abundance of fragments at *m*/*z* 467 and 449 in the spectra of glycolipid Pb-**1** (Figures 6B, 7A,B). A much higher abundance of these ions would be expected if the glycan chain were linear, whereas in the case of the branched structure shown, they would have to arise from C_3PO_3Na and B_3PO_3Na precursors by double cleavage of both nonreducing terminal residues ($Y_{2\alpha}$ and $Y_{2\beta}$), a process which has been known to be disfavored for nonderivatized glycoconjugates (*55*). An analogous process arising from ions C_3 and B_3 should also be disfavored, but ions of *m*/*z* 365 and 347 are still observed, although in low abundance. The presence of these ions can be explained by an alternative fragmentation pathway involving single cleavage of either one of the terminal residues from the C_2 and B_2 trisaccharide precursor ions. An analogous alternative pathway to *m*/*z* 467 and 449 is not available for the phosphorylated glycan precursors C_3PO_3Na and B_3PO_3Na.

With respect to the lipid moiety, the difference in mass between the predominant pseudomolecular ion and the phosphoglycan fragment (665 u) is in each case consistent with a ceramide made up of (t18:0)-4-hydroxy-sphinganine and h24:0 fatty acid.

α-*Mannosidase Treatment of the Glycosylinositol Released from Glycolipid Pb-**2** by Ammonolysis.* Repeated attempts to hydrolyze intact Pb-**2** with α-mannosidases under a variety of conditions were unsuccessful. However, independent, unambiguous confirmation of the anomeric linkages of the two Man*p* residues was obtained by α-mannosidase treatment of the free glycosylinositol GI-**2**. Following extensive digestion, the products were analyzed by two methods chosen to minimize losses from sample transfer and other workup steps. The entire digest, including buffer and enzyme, was lyophilized once, then lyophilized twice more from D_2O, and finally dissolved in this solvent for acquisition of a 1-D proton NMR spectrum. To control for the possible effects of high salt content on the spectrum of the enzyme digest, it was compared with spectra of standards of pure mannose and *myo*-inositol treated in an identical manner. The spectrum of the enzyme digest clearly exhibited resonances virtually identical to those found in the spectra of both free mannose and free *myo*-inositol (Figure 8). No resonances were observed for GI-**2**, nor for any intermediate mannosyl-substituted *myo*-inositol, indicating complete digestion of both Man*p* residues of GI-**2**. Following this, the digest was recovered, reduced with sodium borohydride, and treated for GC-MS analysis of the products as their per-*O*-acetate derivatives. Again, only the hexa-*O*-acetates of mannitol and

Scheme 3: Fragmentation of Pb-**2** under ESI-CID-MS and ESI-CID-MS/CID-MS Conditions[a]

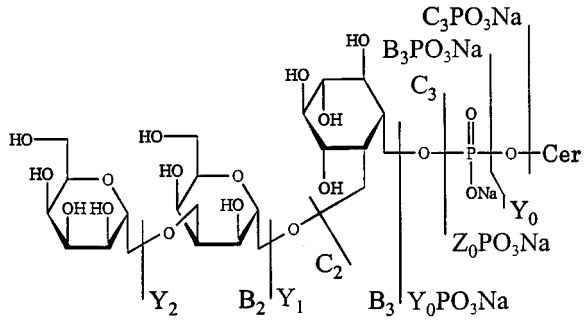

$M+Na^+ = \mathbf{1294}$

[a] Fragment nomenclature is after Domon and Costello (*91*) as applied to glycosylinositol phosphorylceramides in Singh et al. (*89*).

Scheme 4: Fragmentation of Pb-1 under ESI-CID-MS and ESI-CID-MS/CID-MS Conditions.[a]

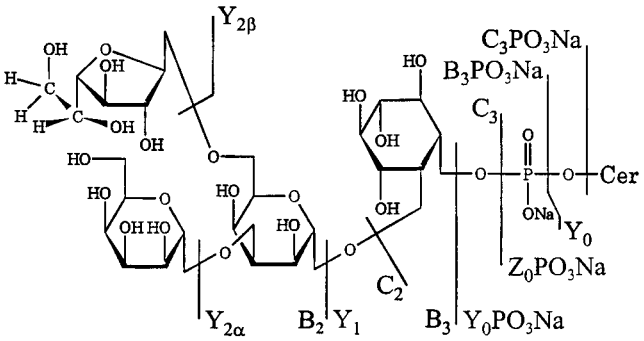

$M+Na^+ = \mathbf{1456}$

[a] Fragment nomenclature is after Domon and Costello (*91*) as applied to glycosylinositol phosphorylceramides in Singh et al. (*89*).

myo-inositol were detected, in a 2:1 ratio. These results confirm the α-configuration of both Man*p* residues of glycolipid Pb-**2** and, by extension, of glycolipid Pb-**1**.

Linkage Analysis by GC-MS. The linkage structure of the terminal trisaccharide of the glycolipid Pb-**1** was confirmed unambiguously by the detection of derivatives for terminal Gal*f* and Man*p* residues (2,3,5,6-tetra-*O*-Me-Gal and 2,3,4,6-tetra-*O*-Me-Man, respectively), along with one for a branching →3[→6]Man*p* residue (2,4-di-*O*-Me-Man). In glycolipid Pb-**2**, the absence of the terminal Gal*f* residue was indicated by deletion of the terminal Gal*f* and →3[→6]Man*p* derivatives from the GC-MS pattern, with the concomitant appearance of a derivative for →3Man*p* (2,4,6-tri-*O*-Me-Man), while that for terminal Man*p* was retained. These data support the proposed linkage of the Gal*f* residue to the 6-position, and the Man*p* to the 3-position, of the branching Man*p* of glycolipid Pb-**1**.

Taken together, the data support the following complete structures for Pb-**1** and Pb-**2**: Pb-**2**, Man*p*α1→3Man*p*α1→2-Ins1-P-1Cer, and Pb-**1**, Man*p*α1→3[Gal*f*β1→6]Man*p*α1→2-Ins1-P-1Cer where the predominant Cer in each consists of t18:0 phytosphingosine and h24:0 fatty acid. These structures are analogous to those of two GIPCs isolated from *H. capsulatum* (*15*): Hc-**V**, Man*p*α1→3Man*p*α1→2 or 6Ins1-P-1Cer, and Hc-**VI**, Man*p*α1→3[Gal*f*α1→6]Man*p*α1→2 or 6Ins1-P-1Cer for which the same Cer structure was found

Table 4: Product Ions Formed in Low-Energy CID Spectra of *P. brasiliensis* Glycosylinositol Phosphorylceramides Pb-2 and Pb-1 (Figures 6 and 7, and Supporting Information)

ion	*m/z* Pb-**2**	Pb-**1**
$[M{\cdot}Na^+]^+$	1294	1456
$[Y_0PO_3Na{\cdot}Na^+]^+$	808	808
$[Z_0PO_3Na{\cdot}Na^+]^+$	790	790
$[Y_0{\cdot}Na^+]^+$	706	706
$[C_3PO_3Na{\cdot}Na^+]^+$	629	791
$[B_3PO_3Na{\cdot}Na^+]^+$	611	773
$[C_3{\cdot}Na^+]^+$	527	689
$[B_3{\cdot}Na^+]^+$	509	671
$[Y_2/C_3PO_3Na{\cdot}Na^+]^+$	467	---
$[Y_{2\alpha\ or\ \beta}/C_3PO_3Na{\cdot}Na^+]^+$	---	629
$[Y_2/B_3PO_3Na{\cdot}Na^+]^+$	449	---
$[Y_{2\alpha\ or\ \beta}/B_3PO_3Na{\cdot}Na^+]^+$	---	611
$[Y_2/C_3{\cdot}Na^+]^+$	365	---
$[Y_{2\alpha\ or\ \beta}/C_3{\cdot}Na^+]^+$	---	527
$[C_2{\cdot}Na^+]^+$	365	527
$[Y_2/B_3{\cdot}Na^+]^+$	347	---
$[Y_{2\alpha\ or\ \beta}/B_3{\cdot}Na^+]^+$	---	509
$[B_2{\cdot}Na^+]^+$	347	509
$[Y_{2\alpha\ or\ \beta}/C_2{\cdot}Na^+]^+$	---	365
$[Y_{2\alpha\ or\ \beta}/B_2{\cdot}Na^+]^+$	---	347
$[Y_1/C_3PO_3Na{\cdot}Na^+]^+$	305	305
$[Y_1/B_3PO_3Na{\cdot}Na^+]^+$	287	287
$[Y_1/C_3{\cdot}Na^+]^+$	203	203
$[Y_1/B_3{\cdot}Na^+]^+$	185	185
$[NaH_2PO_4{\cdot}Na^+]^+$	143	143
$[NaPO_3{\cdot}Na^+]^+$	125	125

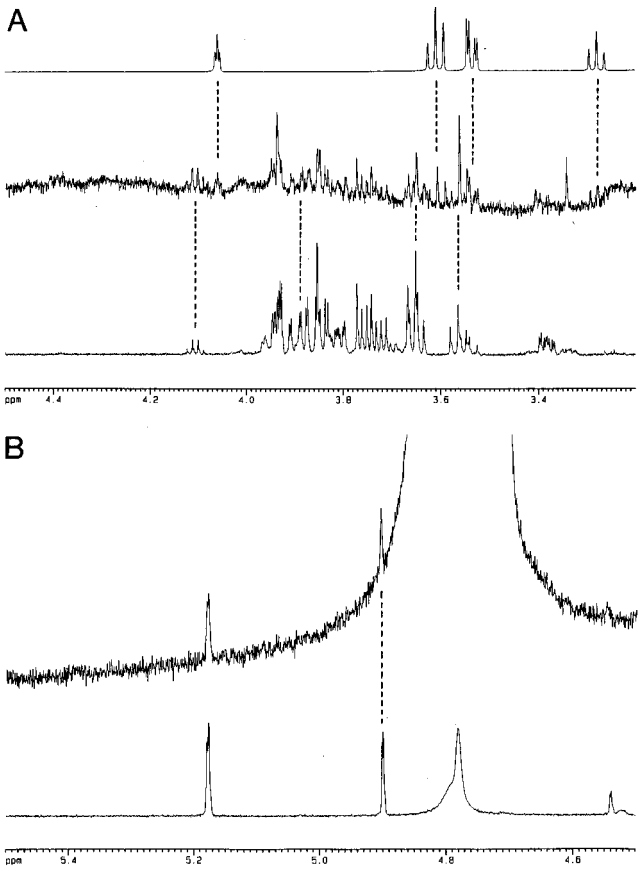

FIGURE 8: Downfield expansion of 1-D proton NMR spectrum of *P. brasiliensis* glycosyliositol GI-**2** following treatment with Jack Bean α-mannosidase, compared with spectra of identically treated *myo*-inositol and mannose. Panel A, 4.5−3.2 ppm region, comparing spectrum of product (Middle) with those of *myo*-inositol (Upper) and mannose (Lower); Panel B, 5.5−4.5 ppm region, comparing spectrum of product (Upper) with that of mannose (Lower). All three spectra were acquired in D_2O at 298 K.

to be predominant. It seems likely that the internal linkage in the *H. capsulatum* antigens is Man*p*α1→2Ins, and that Pb-**2** is identical to Hc-**V**, while Pb-**1** differs from Hc-**VI** only in the anomeric configuration of the terminal galactofuranose residue.

DISCUSSION

Although approximately 12 million patients, mostly farmworkers, are infected by the mycopathogen *P. brasiliensis*, the precise etiology of paracoccidioidomycosis (PCM) is still unclear (*56*, *57*). It is assumed that patients are infected by exposure to the mycelium form, which grows well at 18−24 °C, present in soil (*56*, *58*). Only the yeast form, which grows at 35−37 °C, is detected in patients exhibiting PCM (*59*). Although considerable progress has been made in the diagnosis and treatment of PCM (*60*−*62*), persistent problems exist with respect to antigenic instability (*63*), cross-reactivity and false negative serological results (*64*), and various other types of misdiagnosis (*65*−*68*). In view of the increasing possibility for importation of PCM to non-endemic areas (*66*), as well as the increasing global risk for mycopathogen infection among immunocompromised patients (*69*−*71*), the need for improved methods for diagnosis and treatment of PCM and other fungal diseases is clear. A survey of cell surface membrane components, initiated to identify novel targets for immunodiagnosis and therapy for mycopathogens, led to the structural studies described in this paper.

In addition to glucosylceramides found in the neutral fractions of *P. brasiliensis* glycolipids (*72*), two major glycosylphosphoryl lipids were isolated from the acidic fractions retained by DEAE-Sephadex (*28*, *29*). The sera of all patients with PCM were found to react strongly with one of the acidic components, which was detected in both the yeast and mycelium forms of *P. brasiliensis* (*28*). This component, Pb-**1**, comprised 90−95% of the acidic glycolipids extracted from the yeast form; a second acidic, serologically unreactive glycolipid, Pb-**2**, was a minor component in the yeast form, but was found in amounts comparable to Pb-**1** in the mycelium form. Initial characterization established that the basis for the serological reactivity was a galactofuranose residue present on Pb-**1**. For example, after mild, selective oxidation of this residue with sodium periodate and reduction with sodium borohydride, the reactivity with PCM sera was abolished (*29*). Following acid hydrolysis, the product of the oxidation and reduction was detectable as arabinose (*28*). Of particular interest was the fact that sera from patients with histoplasmosis (HP) failed to react with Pb-**1** (*28*). The basis for this serological distinction is suggested by a comparison of the complete glycan structure of Pb-**1** with that described for Hc-**VI** (*15*), which (assuming the presence of a Manα1→2Ins linkage in the latter) differs only in the anomeric configuration of the galactofuranose residue. After these serological findings, a monoclonal antibody, MEST-1, raised and screened against Pb-**1**, was shown to recognize specifically terminal *β*-galactofuranose residues found in certain mycopathogens and trypanosomatids (*73*, *74*) [for a review of the occurrence of *β*-galactofuranose in glycoconjugates of trypanosomatids, see de Lederkremer and Colli (*75*)]. These results all support the potential utility of free GIPCs as cell surface markers and as elicitors of host immune response.

With respect to understanding the structure and biosynthesis of free GIPCs in *P. brasiliensis* as well as their status in relationship to other fungi, considerable care was exercised to establish as unambiguously as possible the anomeric configuration and location of all glycosyl linkages. This was particularly true in the case of the Manα1→2Ins linkage, which may prove to be fairly general among fungi, although this impression has until now been based for the most part on secondary references (*4*, *7*). The Manα1→2Ins linkage is shared in common with the acylated phospho-*myo*-inositol mannosides (PIMs) (*76*−*78*) which anchor the characteristic lipomannans (LM) and lipoarabinomannans (LAMs) of mycobacteria (*79*−*81*) (recently reviewed, ref *82*). PIM anchors, however, are based on a phosphorylated diacylglycerol (DAG), rather than ceramide, lipid moiety. There is a further interesting divergence between PIMs and the complex fungal GIPCs characterized so far: the long (→6-[Manα→2]Manα1→)$_n$ chains comprising the mannan core of mycobacterial LAMs are attached to the PIM anchor via a Manα1→6Manα→6Ins sequence, while the Man residue linked α→2 to *myo*-inositol remains unsubstituted. In any case, since this linkage is not part of the mammalian repertoire, as far as is known, the as yet unidentified transferase(s) responsible for it may provide a useful target for interference in fungal growth, reproduction, or infectivity, provided it is found to be essential for one or more of these functions.

Compared with the relatively simple phosphosphingolipid structures found in *S. cerevisiae*, *C. albicans*, and *C. utilis* [IPC, MIPC, IPMIPC (*9*, *18*, *19*, *83*−*85*)], the presence in filamentous fungi, such as *A. niger* (*4*), *H. capsulatum* (*15*), and *P. brasiliensis*, of more complex GIPCs suggests the possibility in these species of unique recognition functions based on glycan structure, possibly related to the existence of mycelial forms, or, in the case of the latter two, of thermal dimorphism. Distinct from the use of specific GIPC structures covalently bound to proteins as membrane anchors (*1*), it has been suggested that free IPCs may be required in *S. cerevisiae* as cofactors for proper activation of certain membrane-bound enzymes (*86*); or they may serve "chaperone"-like functions facilitating vesicular transport of proteins (*87*); an interesting further possibility is that the glycans of free GIPCs might take part in noncovalent stabilizing interactions with protein and/or polysaccharide components of the inner cell wall (*4*). Such interactions might require the longer "reach" of IPMIPC, or the more elaborate glycan structures found on complex GIPCs, since it is doubtful that the single Man*p*α1→2 residue of MIPC extends very far from the membrane surface.

Current knowledge of fungal GIPC structure includes a mere handful of species, and most of these fall into two classes within the phylum Ascomycota: *Saccharomyces* and *Candida* are Hemiascomycetes, while *Aspergillus*, *Paracoccidioides*, and *Histoplasma* (*Ajellomyces*), all expressing complex free GIPCs, are Euascomycetes; moreover, the former are both of the order Saccharomycetales, while the latter are all in the same subclass, Plectomycetes. *N. crassa*, from which IPC and (IP)$_2$C have been isolated, but which appears not to express complex GIPCs, is also in the class of Euascomycetes, but in a different subclass, Pyrenomycetes. This rudimentary analysis suggests that complex GIPCs might be significant taxonomic markers. Considering their

potential significance as targets for diagnosis and treatment of fungal disease, the value of further study of GIPC structure, synthesis, and function over a wider spectrum of mycopathogens seems clearly evident.

With respect to the techniques used in this study, we are aware of only one previous NMR characterization of an intact (G)IPC [isolated from *Tritrichomonas foetus* (*88*)]; in this case the ^{1}H chemical shift data were given for a ceramide composed of (d18:1) sphing-4-enine and non-hydroxylated fatty acids, and there is little correlation with those we have now observed for the *P. brasiliensis* GIPCs containing phytosphingosine and 2-hydroxylated fatty acids. We failed at first to recognize the presence of ceramide on the basis of the NMR data alone, partly due to overlap of the residual HOD resonance with crucial correlation peaks connecting the bulk alkyl/acyl ceramide protons with those near the phosphoglycan; and partly due to the lack of prior data on the chemical shifts to be expected for this type of ceramide when phosphorylated at C-1. The identities of the lipid moieties in Pb-**1** and Pb-**2** were initially deduced instead from the ESI-MS data along with the fatty acid and sphingosine component analyses; in general, also, detailed characterization of the chain lengths of the sphingosine and fatty acyl moieties is facilitated by the use of MS and GC-MS techniques, rather than NMR spectroscopy. Previously, both negative and positive ion mode FAB-MS and FAB-MS/CID-MS have been used in the analysis of underivatized free fungal (G)IPCs (*10*−*12*, *48*, *88*, *89*). Negative ion mode ESI-MS was used in the characterization of (G)IPCs from *S. cerevisiae*, but only pseudomolecular ion species were observed ($[M-H]^-$ for IPC and MIPC, $[M-2H]^-$ for IP-MIPC) (*90*). Our results indicate that positive ion mode ESI-MS and ESI-MS/CID-MS are also useful for analysis of this class of compounds. It is hoped that both the NMR and MS data presented in this study will facilitate recognition of GIPCs, including those with highly hydroxylated phosphorylceramides, isolated from other organisms.

ACKNOWLEDGMENT

The authors gratefully acknowledge the technical support of Dr. Tom Pratum (University of Washington NMR Facility) and Dr. John Glushka (Complex Carbohydrate Research Center NMR Facility).

SUPPORTING INFORMATION AVAILABLE

Sections of TOCSY and NOESY spectra for Pb-**2** showing correlations from H-1 of hexose residues; 1-D ^{1}H-detected ^{1}H-^{31}P heteronuclear correlation spectra for Pb-**1** and Pb-**2**; ESI-CID-MS/CID-MS product ion spectra for *m*/*z* 629 (C_3PO_3Na) and 611 (B_3PO_3Na) of Pb-**2** (12 pages). Ordering information is given on any current masthead page.

REFERENCES

1. Conzelmann, A., Puoti, A., Lester, R. L., and Desponds, C. (1992) *EMBO J. 11*, 457−466.
2. Fankhauser, C., Homans, S. W., Thomas-Oates, J. E., Mcconville, M. J., Desponds, C., Conzelmann, A., and Ferguson, M. A. J. (1993) *J. Biol. Chem. 268*, 26365−26374.
3. Kanfer, J. N., and Hakomori, S. (1983) *Sphingolipid Biochemistry*, Plenum Press, New York and London.
4. Brennan, P. J., and Lösel, D. M. (1978) *Adv. Microb. Physiol. 17*, 47−179.
5. Stults, C. L. M., Sweeley, C. C., and Macher, B. A. (1989) *Methods Enzymol. 179*, 167−214.
6. Jin, W., Rinehart, K. L., and Jares-Erijman, E. A. (1994) *J. Org. Chem. 59*, 144−147.
7. Lester, R. L., and Dickson, R. C. (1993) *Adv. Lipid Res. 26*, 253−274.
8. Vincent, V. L., and Klig, L. S. (1995) *Microbiology 141*, 1829−1837.
9. Wells, G. B., Dickson, R. C., and Lester, R. L. (1996) *J. Bacteriol. 178*, 6223−6226.
10. Lhomme, O., Bruneteau, M., Costello, C. E., Mas, P., Molot, P.-M., Dell, A., Tiller, P. R., and Michel, G. (1990) *Eur. J. Biochem. 191*, 203−209.
11. Pivot, V., Bruneteau, M., Mas, P., Bompeix, G., and Michel, G. (1994) *Lipids 29*, 21−25.
12. Bruneteau, M., Fournol, F., Gandon, C., Becchi, M., and Pivot, V. (1997) *Lipids 32*, 359−362.
13. Lester, R. L., Smith, S. W., Wells, G. B., Rees, D. C., and Angus, W. W. (1974) *J. Biol. Chem. 249*, 3388−3394.
14. Barr, K., and Lester, R. L. (1984) *Biochemistry 23*, 5581−5588.
15. Barr, K., Laine, R. A., and Lester, R. L. (1984) *Biochemistry 23*, 5589−5596.
16. Brennan, P. J., and Roe, J. (1975) *Biochem. J. 147*, 179−180.
17. Byrne, P. F., and Brennan, P. J. (1976) *Biochem. Soc. Trans. 4*, 893−895.
18. Wagner, H., and Zofcsik, W. (1966) *Biochem. Z. 344*, 314−316.
19. Wagner, H., and Zofcsik, W. (1966) *Biochem. Z. 346*, 350.
20. Franco, M. (1987) *J. Med. Vet. Mycol. 25*, 5−18.
21. Franco, M., Peracoli, M. T., Soares, A., Montenegro, R., Mendes, R. P., and Meira, D. A. (1993) *Curr. Top. Med. Mycol. 5*, 115−149.
22. Medoff, G., Painter, A., and Kobayashi, G. S. (1987) *J. Bacteriol. 169*, 4055−4060.
23. San-Blas, G. (1993) *Arch. Med. Res. 24*, 267−268.
24. Fulciniti, F., Troncone, G., Fazioli, F., Vetrani, A., Zeppa, P., Manco, A., and Palombini, L. (1996) *Diagn. Cytopathol. 15*, 442−446.
25. McGinnis, M. R. (1983) *Am. J. Med. 75*, 129−138.
26. Pacheco, R. A., Arruda, W. O., Hunhevicz, S. C., Tsubouchi, M. H., and Torres, L. F. (1996) *Arq. Neuro-psiquiatr. 54*, 474−478.
27. Colli, B. O., Assirati, J. A., Jr, Machado, H. R., Figueiredo, J. F., Chimelli, L., Salvarani, C. P., and Dos Santos, F. (1996) *Arq. Neuro-psiquiatr. 54*, 466−473.
28. Toledo, M. S., Suzuki, E., Straus, A. H., and Takahashi, H. K. (1995) *J. Med. Vet. Mycol. 33*, 247−251.
29. Levery, S. B., Toledo, M. S., Suzuki, E., Salyan, M. E., Hakomori, S., Straus, A. H., and Takahashi, H. K. (1996) *Biochem. Biophys. Res. Commun. 222*, 639−645.
30. Straus, A. H., Levery, S. B., Jasiulionis, M. G., Salyan, M. E., Steele, S. J., Travassos, L. R., Hakomori, S., and Takahashi, H. K. (1993) *J. Biol. Chem. 268*, 13723−13730.
31. Bax, A., Griffey, R. H., and Hawkins, B. L. (1983) *J. Magn. Reson. 55*, 301−315.
32. Dabrowski, J., Hanfland, P., and Egge, H. (1980) *Biochemistry 19*, 5652−5658.
33. Piantini, U., Sorensen, O. W., and Ernst, R. R. (1982) *J. Am. Chem. Soc. 104*, 6800−6801.
34. Rance, M., Sorensen, O. W., Bodenhausen, G., Wagner, G., Ernst, R. R., and Wüthrich, K. (1983) *Biochem. Biophys. Res. Commun. 117*, 479−485.
35. Braunschweiler, L., and Ernst, R. R. (1983) *J. Magn. Reson. 53*, 521−528.
36. Bax, A., and Davis, D. G. (1985) *J. Magn. Reson. 65*, 355−360.
37. Marion, D., and Wüthrich, K. (1983) *Biochem. Biophys. Res. Commun. 113*, 967−974.
38. Bodenhausen, G., Kogler, H., and Ernst, R. R. (1984) *J. Magn. Reson. 58*, 370−388.
39. Levery, S. B., Holmes, E. H., Harris, D. D., and Hakomori, S. (1992) *Biochemistry 31*, 1069−1080.

40. Eich, G., Bodenhausen, G., and Ernst, R. R. (1982) *J. Am. Chem. Soc. 104*, 3731−3732.
41. Bax, A., and Drobny, G. (1985) *J. Magn. Reson. 61*, 306−320.
42. Merkle, R. K., and Poppe, I. (1994) *Methods Enzymol. 230*, 1−15.
43. Sweeley, C. C., and Moscatelli, E. A. (1959) *J. Lipid Res. 1*, 40−47.
44. Gaver, R. C., and Sweeley, C. C. (1965) *J. Am. Oil Chem. Soc. 42*, 294−298.
45. Levery, S. B., and Hakomori, S. (1987) *Methods Enzymol. 138*, 13−25.
46. Björndal, H., Hellerqvist, C. G., Lindberg, B., and Svensson, S. (1970) *Angew. Chem., Int. Ed. Engl. 9*, 610−619.
47. Jansson, P.-E., Kenne, L., Liedgren, H., Lindberg, B., and Lönngren, J. (1976) *Chem. Commun. (Stockholm Univ.)* 1−75.
48. Costello, C. E., and Vath, J. E. (1990) *Methods Enzymol. 193*, 738−768.
49. Dell, A. (1987) *Adv. Carbohydr. Chem. Biochem. 45*, 19−72.
50. Thorpe, S. R., and Sweeley, C. C. (1967) *Biochemistry 6*, 887−897.
51. Vliegenthart, J. F. G., Dorland, L., and van Halbeek, H. (1983) *Adv. Carbohydr. Chem. Biochem. 41*, 209−374.
52. Verostek, M. F., Atkinson, P. H., and Trimble, R. B. (1993) *J. Biol. Chem. 268*, 12104−12115.
53. Gerwig, G. J., de Waard, P., Kamerling, J. P., Vliegenthart, J. F. G., Morgenstern, E., Lamed, R., and Bayer, E. A. (1989) *J. Biol. Chem. 264*, 1027−1035.
54. Angyal, S. J. (1979) *Carbohydr. Res. 77*, 37−50.
55. Webb, J. W., Jiang, K., Gillece-Castro, B. L., Tarentino, A. L., Plummer, T. H., Byrd, J. C., Fisher, S. J., and Burlingame, A. L. (1988) *Anal. Biochem. 169*, 337−349.
56. Restrepo, A. (1985) *Sabouraudia 23*, 323−334.
57. McEwen, J. G., Garcia, A. M., Ortiz, B. L., Botero, S., and Restrepo, A. (1995) *Arch. Med. Res. 26*, 305−306.
58. Negroni, P. (1966) *Prensa Med. Argent. 53*, 2381−2382.
59. San-Blas, G. (1993) *J. Med. Vet. Mycol. 31*, 99−113.
60. Taborda, C. P., and Camargo, Z. P. (1993) *J. Med. Vet. Mycol. 31*, 155−160.
61. Brummer, E., Castaneda, E., and Restrepo, A. (1993) *Clin. Microbiol. Rev. 6*, 89−117.
62. Straus, A. H., Freymuller, E., Travassos, L. R., and Takahashi, H. K. (1996) *J. Med. Vet. Mycol. 34*, 181−186.
63. Franco, M., Bagagli, E., Cunha, M., Chamma, L. G., and Fecchio, D. (1996) *Mycopathologia 135*, 13−19.
64. del Negro, G. M., Benard, G., de Assis, C. M., Vidal, M. S., Garcia, N. M., Otani, C., Shikanai-Yasuda, M. A., and da S. Lacaz, C. (1995) *J. Med. Vet. Mycol. 33*, 113−116.
65. Penna, F. J. (1979) *Gut 20*, 896−899.
66. Ajello, L., and Polonelli, L. (1985) *Eur. J. Epidemiol. 1*, 160−165.
67. Cooper, B. H. (1987) *Mycopathologia 97*, 189−193.
68. Siletti, R. P., Glezerov, V., and Schwartz, I. S. (1996) *J. Clin. Microbiol. 34*, 2328−2330.
69. Shikanai-Yasuda, M. A., Duarte, M. I., Nunes, D. F., Lacaz, C. S., Sabagga, E., Abdala, E., Duarte, A. J., and Lopes, M. H. (1995) *J. Med. Vet. Mycol. 33*, 411−414.
70. Reis, M. A., Costa, R. S., and Ferraz, A. S. (1995) *J. R. Soc. Med. 88*, 24−27.
71. Goldani, L. Z., and Sugar, A. M. (1995) *Clin. Infect. Dis. 21*, 1275−1281.
72. Takahashi, H. K., Levery, S. B., Toledo, M. S., Suzuki, E., Salyan, M. E., Hakomori, S., and Straus, A. H. (1996) *Braz. J. Med. Biol. Res. 29*, 1441−1444.
73. Straus, A. H., Suzuki, E., Toledo, M. S., Takizawa, C. M., and Takahashi, H. K. (1995) *Braz. J. Med. Biol. Res. 28*, 919−923.
74. Suzuki, E., Toledo, M. S., Takahashi, H. K., and Straus, A. H. (1997) *Glycobiology 7*, 463−468.
75. de Lederkremer, R. M., and Colli, W. (1995) *Glycobiology 5*, 547−552.
76. Lee, Y. C., and Ballou, C. E. (1964) *J. Biol. Chem. 239*, 1316−1327.
77. Lee, Y. C., and Ballou, C. E. (1965) *Biochemistry 4*, 1395−1404.
78. Khoo, K. H., Dell, A., Morris, H. R., Brennan, P. J., and Chatterjee, D. (1995) *Glycobiology 5*, 117−127.
79. Hunter, S. W., and Brennan, P. J. (1990) *J. Biol. Chem. 265*, 9272−9279.
80. Chatterjee, D., Hunter, S. W., McNeil, M., and Brennan, P. J. (1992) *J. Biol. Chem. 267*, 6228−6233.
81. Nigou, J., Gilleron, M., Cahuzac, B., Bounery, J. D., Herold, M., Thurnher, M., and Puzo, G. (1997) *J. Biol. Chem. 272*, 23094−23103.
82. Chatterjee, D., and Khoo, K. H. (1998) *Glycobiology 8*, 113−120.
83. Steiner, S., Smith, S. W., Waechter, C. J., and Lester, R. L. (1969) *Proc. Natl. Acad. Sci. U.S.A. 64*, 1042−1048.
84. Smith, S. W., and Lester, R. L. (1974) *J. Biol. Chem. 249*, 3395−3405.
85. Wells, G. B., and Lester, R. L. (1983) *J. Biol. Chem. 258*, 10200−10203.
86. Patton, J. L., and Lester, R. L. (1992) *Arch. Biochem. Biophys. 292*, 70−76.
87. Skrzypek, M., Lester, R. L., and Dickson, R. C. (1997) *J. Bacteriol. 179*, 1513−1520.
88. Costello, C. E., Glushka, J., van Halbeek, H., and Singh, B. N. (1993) *Glycobiology 3*, 261−269.
89. Singh, B. N., Costello, C. E., and Beach, D. H. (1991) *Arch. Biochem. Biophys. 286*, 409−418.
90. Hechtberger, P., Zinser, E., Saf, R., Hummel, K., Paltauf, F., and Daum, G. (1994) *Eur. J. Biochem. 225*, 641−649.
91. Domon, B., and Costello, C. E. (1988) *Glycoconjugate J. 5*, 397−409

BI9730083